



Optimizing interfacial process of Mg metal anode by porphyrin adsorption layer in Cl-free conventional electrolyte

Yichao Zhuang, Jiayue Wu, Haiming Hua, Fei Wang, Dongzheng Wu, Yaoqi Xu, Jing Zeng*, Jinbao Zhao*

College of Chemistry and Chemical Engineering, State-Province Joint Engineering Laboratory of Power Source Technology for New Energy Vehicle, State Key Laboratory of Physical Chemistry of Solid Surfaces, Engineering Research Center of Electrochemical Technology, Ministry of Education, Collaborative Innovation Center of Chemistry for Energy Materials, Xiamen University, Xiamen 361005, China

ARTICLE INFO

Keywords:

Mg metal anode
Cl-free conventional electrolyte
Adsorption layer
Mg²⁺ solvation optimization

ABSTRACT

The viability of Mg metal batteries is severely threatened by the passivating instinct of Mg metal in Cl-free conventional electrolytes. To realize the reversible Mg stripping/plating in the conventional electrolyte, 5,10,15,20-tetraphenylporphyrin (TPP) with planar structure and strong adsorption ability is added into electrolyte to optimize the interfacial process by constructing a dynamic molecular adsorption layer on Mg anode, which is different from the method of tailoring artificial solid electrolyte interphases to facilitate Mg²⁺ transport. On one side, TPP molecules served as a protective layer to avoid the direct contact between Mg anode and passivation-inducing factors from electrolyte, alleviating passivation effectively. On the other side, a locally high concentration of TPP is created near the Mg surface for Mg²⁺ solvation sheath reorganization. Theoretical calculations verify that [MgTPP(DME)₂] in TPP-containing electrolyte possesses higher stability and a lower energy barrier than [Mg(DME)₃]²⁺ during desolvation, further alleviating passivation and reducing the overpotential of Mg metal. Consequently, the Mg symmetrical battery exhibits a reduced polarization voltage of 0.6 V from ~ 2 V and a longer cycling life of over 500 h. With TPP-containing electrolyte, the Mg||V₂O₅ full battery presents a higher initial capacity of 186.5 mAh/g, which confirms the practicability of this additive strategy.

1. Introduction

As a promising energy storage device, lithium-ion batteries (LIBs) have been integrated into human life and production. However, the limited energy density and scarcity of lithium resource restricted the further development of LIBs. To meet the upgrowing demand for battery quantity and energy density, post-lithium batteries are being pursued [1–4]. Among the post-lithium-ion batteries, rechargeable Mg metal batteries have drawn researchers' attention due to their potential advantages of low cost, high safety and high specific capacity [5–10]. Nevertheless, a fatal problem of Mg metal batteries is the absence of suitable electrolyte system [11]. For example, magnesium bis(trifluoromethanesulfonyl) imide (Mg(TFSI)₂) is an extensive studied conventional electrolyte salt due to its high ionic conductivity, wide electrochemical window and high thermal stability, and its production process can be referred from the LIBs electrolyte existed [12]. In commonly investigated Mg(TFSI)₂/1,2-dimethoxyethane (DME) electrolyte, however, anion [13], solvents [14,15] and contaminants such as

water [12,16] are all passivation-inducing factors which can react with Mg and form a passivation film with sluggish Mg²⁺ diffusion, causing the excessively high overpotential of Mg stripping/plating and the failure of Mg metal battery [16–19]. During the last few decades, researchers employ the electrolyte containing Cl or other halogens, such as the magnesium halo-alkyl aluminate complex electrolytes [20], to interdict the side reactions through adsorbing on Mg surface and blocking the passivation-inducing factors [21,22]. Although the presence of Cl overcomes the high overpotential of Mg stripping/plating, it also causes the problems of Cl⁻ corrosion [23,24] and high disassociation energy of Mg-Cl bond [25], restricting its further application in actual battery systems. Therefore, the Cl-free Mg metal battery systems with ameliorated electrolyte-anode interphase are highly desired.

Since Ban et al. originally constructed an artificial interphase consisting of polyacrylonitrile and Mg(CF₃SO₃)₂ on Mg powder to reduce the Mg anode overpotential [26], several novel artificial solid electrolyte interphases (SEI) for Cl-free electrolyte have been fabricated to separate passivation-inducing factors from electrolyte-anode interphase in recent

* Corresponding authors.

E-mail addresses: zengjing@xmu.edu.cn (J. Zeng), jbzha@xmu.edu.cn (J. Zhao).

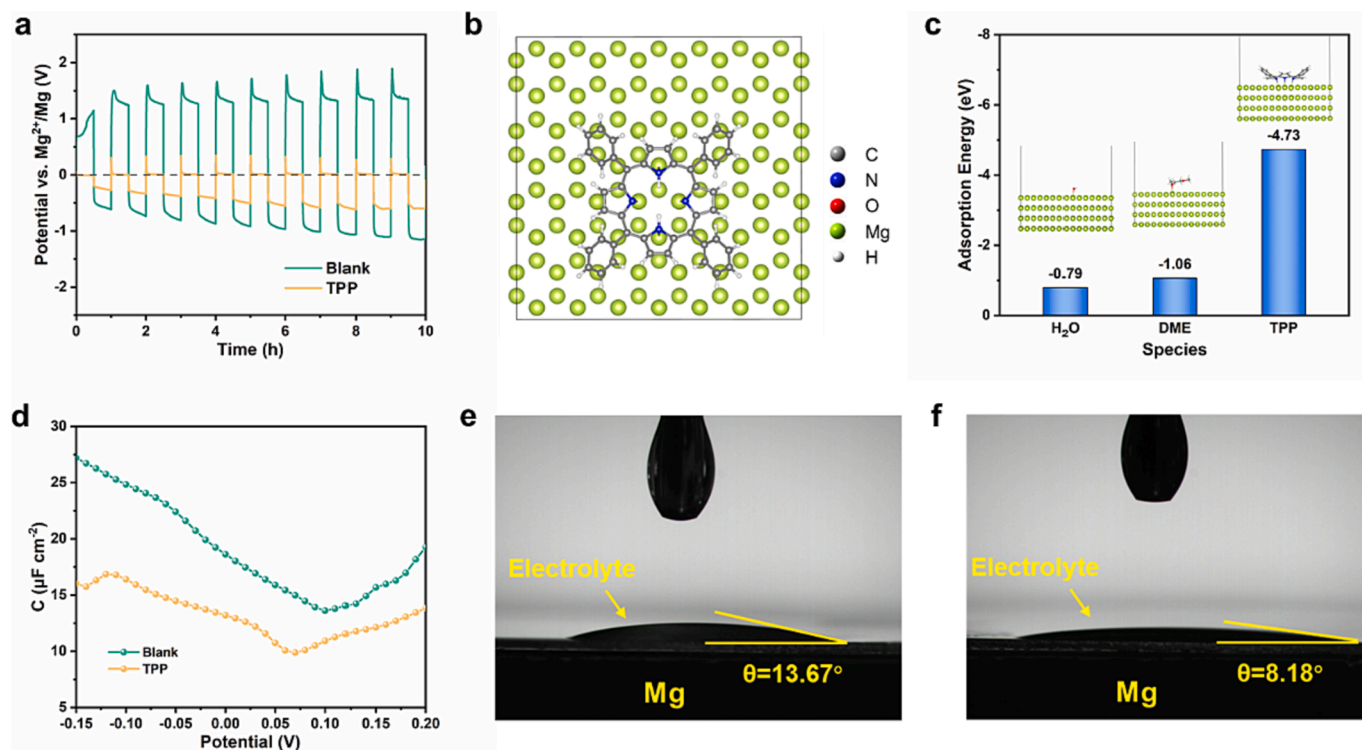


Fig. 1. (a) Voltage profiles of the three-electrode system with different electrolytes. The work, counter and reference electrodes are all Mg foils. (b) The adsorption of TPP molecule with Mg (001) in top view. (c) The adsorption energy of Mg (001) with H₂O, DME and TPP molecule. (d) Differential capacitance curves measured at 298 K with 0.3 M Mg(TFSI)₂/DME and 0.3 M Mg(TFSI)₂/DME + 0.02 M TPP. Contact angles of (e) 0.3 M Mg(TFSI)₂/DME and (f) 0.3 M Mg(TFSI)₂/DME + 0.02 M TPP on Mg anode.

years [27–31]. However, artificial SEI obtained by ex-situ methods tends to be unstable under long term cycling due to volume expansion, and inevitably complicates the production process of Mg metal batteries [32]. The interfacial adsorption layer formed on the Mg anode through the electrolyte additive strategy can also evade the occurrence of side reactions [33]. Yang et al. introduced 1-butyl-1-methylpyrrolidinium cation (Pyr₁₄⁺) into the Mg(TFSI)₂/DME electrolyte to realize uniform plating via an electrostatic shielding strategy [34]. Again, based on the higher adsorption energy of aniline, Yang et al. tailored a non-passive interphase consisting of aniline and much fewer by-products on Mg [35]. Nevertheless, current studies tend to focus on the formation of protective layers on the surface of Mg metal to interdict the side reactions and alleviate the passivation phenomenon, while ignore the Mg anode may still suffer from inferior plating dynamics caused by the high desolvation energy barrier of $[\text{Mg}(\text{DME})_3]^{2+}$. The recent researches show that the optimization of solvation sheath through adding massive novel solvent, such as methoxyethyl-amine chelants [36] or organophosphorus [37], is an effective method to realize superior interfacial reaction dynamics. Our group also proposed the unique solvated structure of Mg^{2+} in Mg(TFSI)₂/3-methoxypropylamine electrolyte, which leads to the fast charge transfer kinetics during Mg stripping/plating [15].

Herein, based on the strong adsorption effect and close interaction with Mg^{2+} of N element, a planar molecule with 4 N atoms, 5,10,15,20-tetraphenylporphyrin (TPP), is applied as effective bifunctional additive to optimize interfacial reactions. As a planar molecule with 4 N atoms, TPP can be strongly adsorbed onto Mg anode and constitute a uniform molecular coating layer to homogenize the distribution of Mg^{2+} . In this study, it is demonstrated that only a small amount of TPP (1.2 wt%) can modify the electrolyte-anode interphase and improve the stripping/plating process of Mg anode effectively. The enhanced electrochemical performances of Mg symmetric cell and Mg||V₂O₅ full battery are both exhibited. The functions of TPP molecules are verified through

experiments and theoretical calculations. On one hand, the adsorption of TPP can shield the Mg anode from the attack of the passivation-inducing factors, resulting in slower side reactions and fewer by-products. On the other hand, the adsorption of TPP creates a locally high concentration of TPP on Mg anode [38,39], optimizing the solvation sheath of Mg^{2+} near the surface and reducing plating overpotential.

2. Result and discussion

Firstly, to study the effect of TPP on Mg stripping/plating, the overpotentials of Mg stripping and plating are separated by a three-electrode system. Fig. 1a shows the Mg overpotential profiles of the three-electrode system with different electrolytes. It is speculated that the overpotential of stripping process is contributed by the energy barrier of Mg^{2+} across the passivation film from metal substrate to electrolyte [40], while the plating process is contributed by the energy barrier of de-solvation of Mg^{2+} and Mg^{2+} across the passivation film in the opposite direction. During the first stripping process in blank electrolyte, the grown passivation inhibits the transport of Mg^{2+} and raise its overpotential to 1.147 V. However, the overpotential of the first plating in blank electrolyte is only 0.616 V, lower than that for the stripping process. The process of Mg^{2+} across the passivation film from electrolyte to metal substrate might not happen since Mg^{2+} can obtain electrons from passivation film more easily. A mosaic-type electrodeposits have been found in conventional electrolyte to support this speculation [12]. In contrast, after the addition of TPP, the Mg stripping overpotential of Mg decreased to 0.065 V and plating overpotential is reduced to 0.272 V, suggesting passivation on Mg has been significantly alleviated. The voltage profiles of TPP-containing electrolyte manifest that the addition of TPP can improve the stripping and plating process of Mg simultaneously.

To explain the mechanism that how TPP improves Mg stripping/plating process, the adsorption behavior of TPP molecules on Mg is

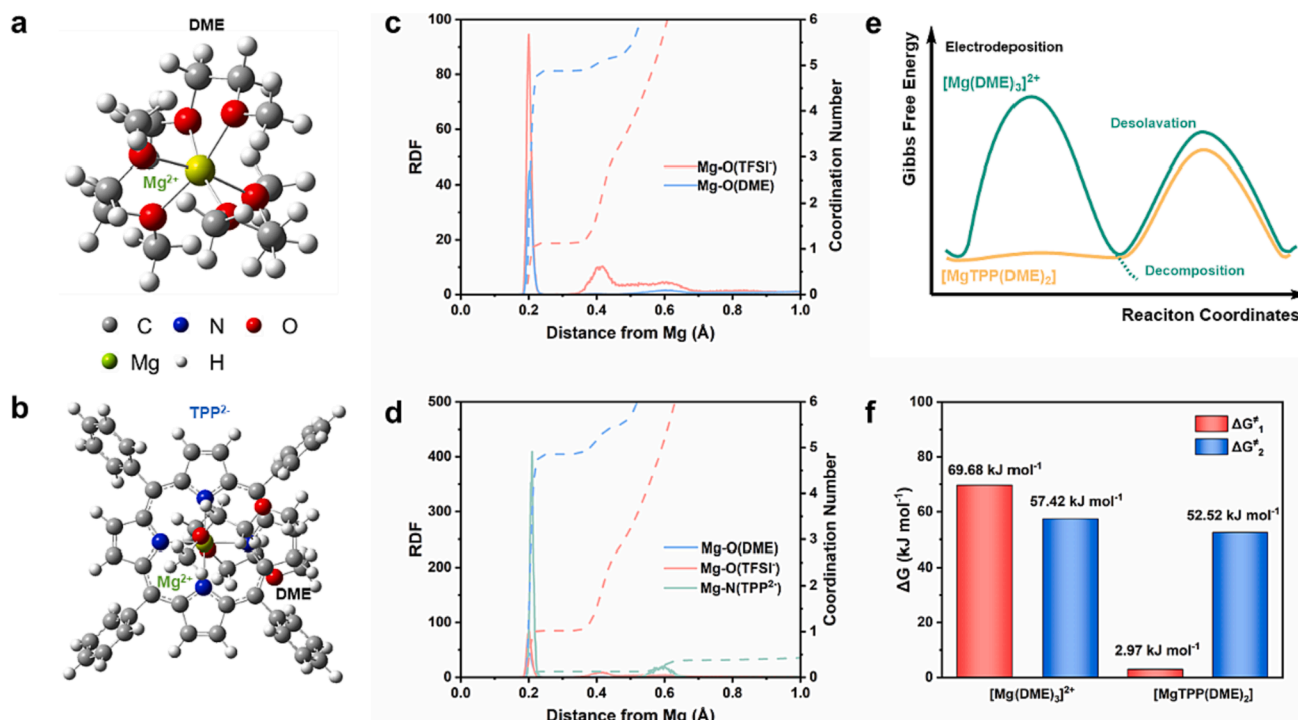


Fig. 2. The geometric structure of (a) $[\text{Mg}(\text{DME})_3]^{2+}$ and (b) $[\text{MgTPP}(\text{DME})_2]$. The radial distribution functions (RDFs) of (c) 0.3 M $\text{Mg}(\text{TFSI})_2/\text{DME}$ and (d) 0.3 M $\text{Mg}(\text{TFSI})_2/\text{DME} + 0.02$ M TPP electrolyte. (e) The Gibbs free energy curves of the interface electrochemical reaction process for $[\text{Mg}(\text{DME})_3]^{2+}$ and $[\text{MgTPP}(\text{DME})_2]$. (f) The Gibbs activation free energy change of $[\text{Mg}(\text{DME})_3]^{2+}$ and $[\text{MgTPP}(\text{DME})_2]$ during the two steps interface electrochemical reaction.

investigated initially. As illustrated in Fig. 1b, c and S1, TPP is adsorbed in a parallel manner on the Mg surface with an adsorption energy of -4.72 eV, much higher than that for H_2O (-0.79 eV) and DME (-1.06 eV). Such a high adsorption energy represents that TPP are strongly inclined to accumulate on the Mg surface and reduce the contact between the passivation-inducing factors (TFSI, DME and H_2O) and the Mg anode.

The adsorption behavior of TPP can be confirmed by differential capacitance curves in Fig. 1d [41,42]. Due to the adsorption of TPP molecular with lower permittivity, the differential capacitance near the point of zero charge (PZC) is significantly reduced. Besides, with the increase of the concentration of TPP, the decrease of the electrolyte contact angle on Mg can also reflect the magnesiophilic property of TPP

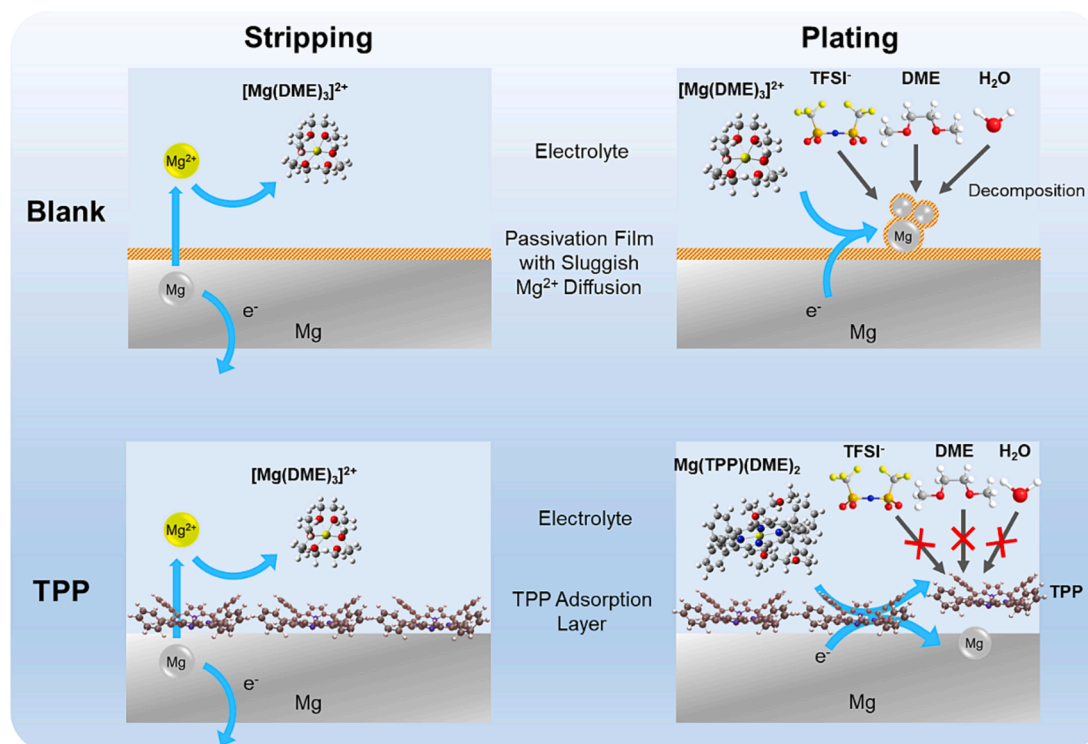


Fig. 3. Illustration of Mg stripping/plating in the different electrolytes.

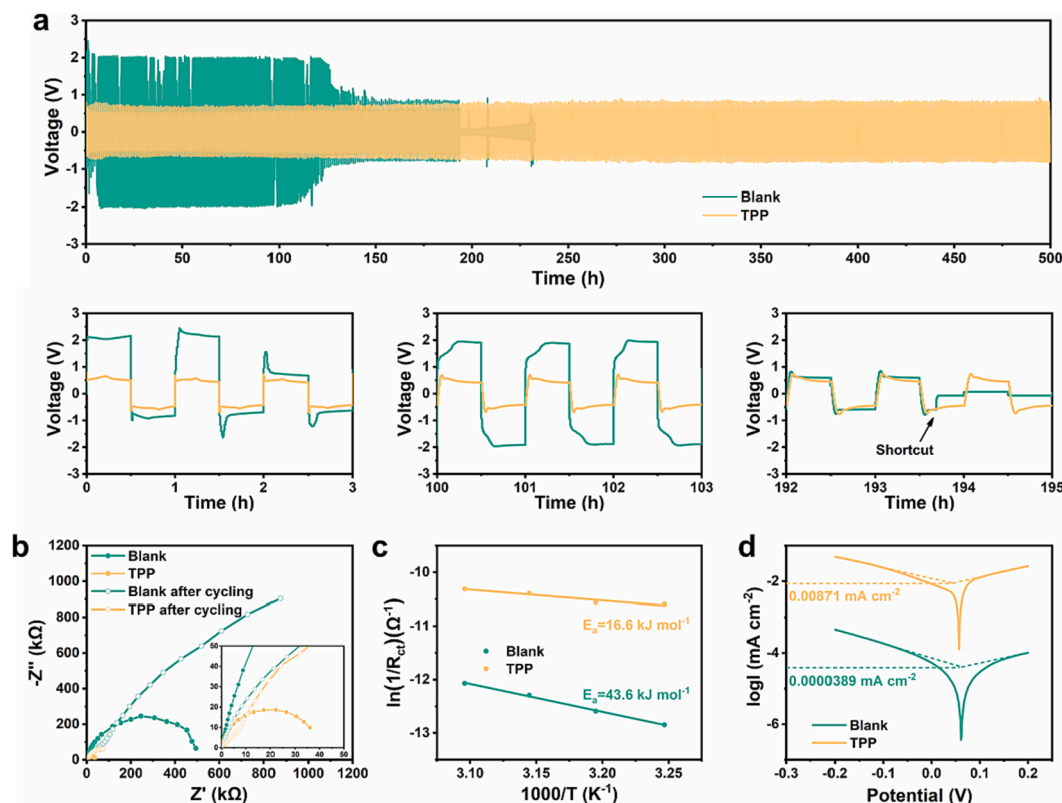


Fig. 4. (a) The galvanostatic voltage profiles of Mg symmetric cells with 0.3 M Mg(TFSI)₂/DME and 0.3 M Mg(TFSI)₂/DME + 0.02 M TPP at 0.01 mA cm⁻². (b) EIS spectra of fresh and cycled Mg symmetric cells with different electrolytes. (c) Fitting curves of interfacial resistance's Napierian logarithm versus reciprocal temperature for Mg symmetric cells with different electrolytes. (d) Tafel plot of Mg symmetric cells with different electrolytes.

molecule (Fig. 1 e-f and S2). The smaller contact angle of TPP-containing electrolyte implies its better wettability on Mg metal, which is conducive to the smooth deposition of Mg. The adsorption of TPP on the Mg metal can not only protect Mg anode from exposure to passivation-inducing factors, but also create a locally high concentration of TPP near the surface.

The improvement of plating process brought by TPP is analyzed by studying Mg²⁺ solvated structures in TPP-containing electrolyte. The speculated Mg²⁺ solvated geometric structures are illustrated in Fig. 2a and 2b. To verify the rationality of speculated structures, a classical molecular dynamic (CMD) simulation is carried out and displayed in Fig. 2c, 2d and S3. The results show that compared to the [Mg(DME)₃]²⁺ formed in the blank electrolyte, the new solvated structure [MgTPP(DME)₂] is formed by the substitution of TPP for DME due to the introduction of the highly electronegative N in the TPP. The simulation results are perfectly agreed with the speculated Mg²⁺ solvated structures. UV/Vis spectra of TPP solutions are also measured to demonstrate the coordination of TPP to Mg²⁺ (Fig. S4). The obvious hyperchromic effect can be observed in TPP solution after the introduction of Mg²⁺, which implies the enhancement of conjugative effect of porphyrin ring and the formation of [MgTPP(DME)₂]. Despite the low concentration of TPP, the TPP molecules adsorbed near the Mg metal creates a locally high concentrations of [MgTPP(DME)₂], which is sufficient to optimize the Mg plating process.

Subsequently, according to previous work in our group [15], the desolvation energy barriers [Mg(DME)₃]²⁺ and [MgTPP(DME)₂] are calculated from the energy value differences between their solvated structure and desolvated structure. The Gibbs activation free energy change during desolvation process is split into two steps: difference between the state before and after the electron transition (ΔG_1^\ddagger), and between the state before and after the solvent dissociation (ΔG_2^\ddagger). The Gibbs free energy curves of the interfacial electrochemical deposition

reaction process for [Mg(DME)₃]²⁺ and [MgTPP(DME)₂] clusters are exhibited in Fig. 2e. For the [Mg(DME)₃]²⁺ cluster, the C – O bond of the DME molecule is lengthen and weaken dramatically during the electron transition process, implying that the DME molecule is prone to decompose via a C – O bond cleavage. In this case, another undecomposed DME molecule is dissociated from the cluster to calculate the ΔG_2^\ddagger . By contrast, [MgTPP(DME)₂] cluster shows high stability during the electron transition process, preventing the manufacture of by-product during Mg plating. In general (Fig. 2f), compared with [Mg(DME)₃]²⁺ (69.68 kJ mol⁻¹), the Gibbs activation free energy of [MgTPP(DME)₂] during the whole interfacial electrochemical reaction process (52.52 kJ mol⁻¹) is reduced, further clarifying the decrease of Mg plating overpotential.

According to the experimental and computational analysis above, the mechanism of Mg stripping/plating in blank and TPP-containing electrolytes is illustrated in Fig. 3. In the blank electrolyte, Mg metal reacts with TFSI, DME and H₂O etc. and forms passivation film on the interphase. Due to high charge density of Mg²⁺, it has stronger interaction with the lattice during the solid diffusion, thus the transport of Mg²⁺ from Mg substrate to electrolyte is seriously hampered and the overpotential of Mg stripping process is extremely high. As for the Mg plating process, electrons can get through the passivation film more easily than Mg²⁺, so Mg is plated on the passivation film rather than beneath it. Besides, DME coordinated with Mg²⁺ tends to decompose during charge transfer process, further exacerbating the passivation degree of Mg surface. The plated Mg would continue to be passivated, leading to uneven deposition and eventually penetrating separator. While the TPP molecules in electrolyte adsorbed strongly on Mg surface and prevent TFSI, DME and H₂O etc. from contacting with the Mg anode directly. The decomposition of electrolyte is alleviated, and passivation is inhibited, thus the Mg stripping overpotential falls to near 0 V. The adsorption of TPP also created a locally high concentration of TPP near

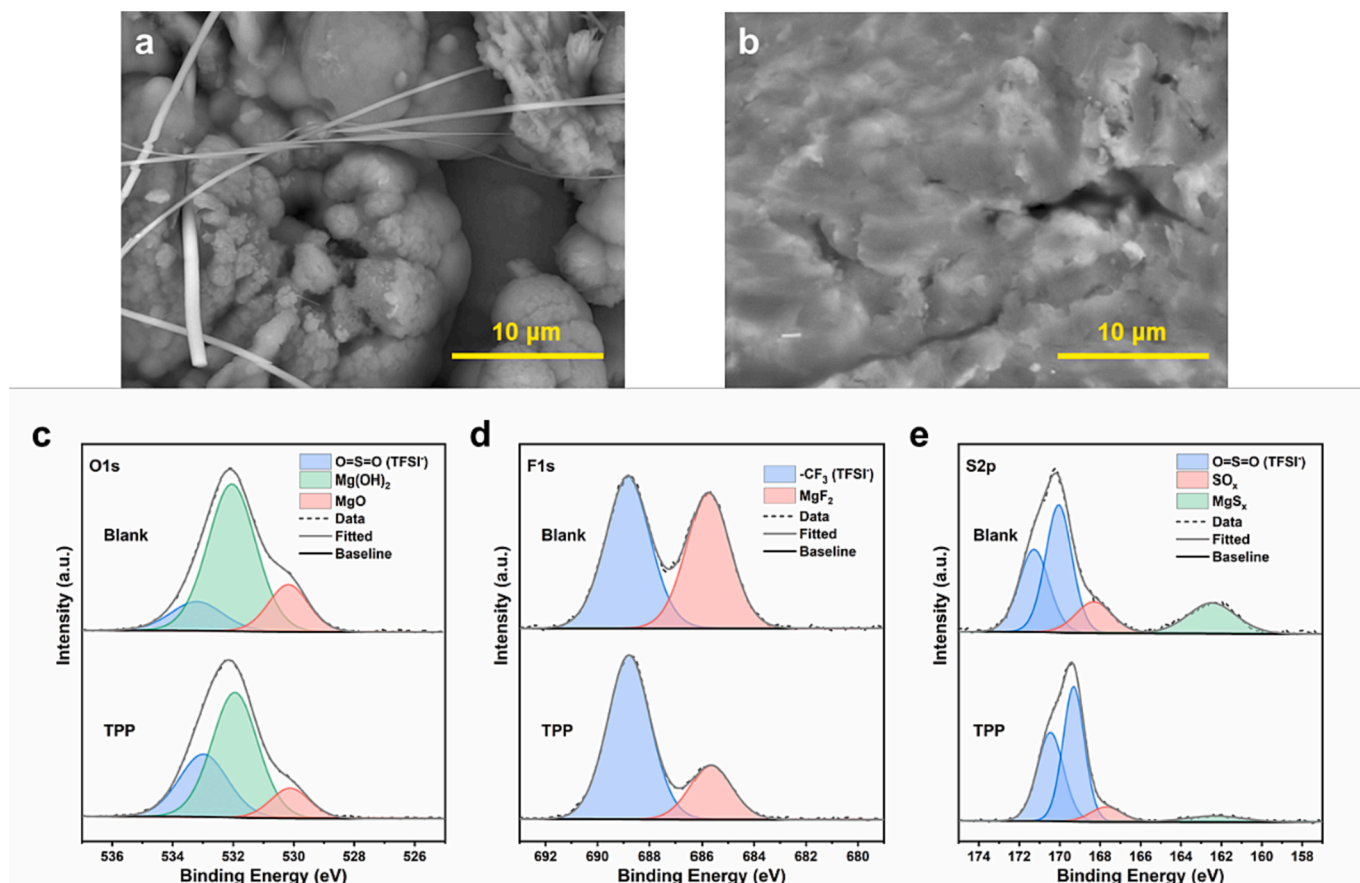


Fig. 5. Surface SEM images of Mg electrode after cycled in (a) 0.3 M Mg(TFSI)₂/DME and (b) 0.3 M Mg(TFSI)₂/DME + 0.02 M TPP. High-resolution XPS (c) O 1s, (d) F 1s, (e) S 2p spectra of Mg electrodes after cycled in different electrolytes.

the Mg surface, forming massive [Mg(TPP)(DME)₂] structures. The existence of [Mg(TPP)(DME)₂] structures not only replaces the unstable [Mg(DME)₃]²⁺ for deposition, but also lowers the energy barrier during desolvation process. After the desolvation of Mg²⁺ is completed, the uncoordinated TPP will be adsorbed on the Mg metal surface to prevent passivation.

The effect of TPP additive in Mg(TFSI)₂/DME electrolyte is estimated by the electrochemical test of Mg symmetric cells. As shown in Fig. 4a, Mg symmetric cell with blank Mg(TFSI)₂/DME electrolyte possesses a large voltage hysteresis of nearly 2 V, which is caused by the passivation of anode-electrolyte interphase. After less than 200 h of cycling, there is a short circuit inside the Mg symmetric cell due to the uneven deposition triggered by passivation. In addition, several suddenly dropped in the polarization voltage can be seen on the voltage profiles of the blank electrolyte, implying the instability of the anode-electrolyte interphase. After adding a small amount of TPP into Mg(TFSI)₂/DME, the polarization voltage of symmetric cells reduce significantly to a stable level of around 0.6 V and lifespan is extended to over 500 h. Fig. 4b is the EIS spectra of fresh and cycled Mg symmetric cells with different electrolytes. The local enlarged EIS spectra shown in Fig. S5a exhibit a characteristic “small semicircle”, which represents the resistance of Mg²⁺ through the SEI, in the high frequency region of Nyquist plots for the electrolyte with TPP, implying that TPP forms a stable and efficient interphase between the anode and electrolyte. Based on the inference above, the Nyquist plots of different electrolytes are fitted as the equivalent circuit model in Fig. S5b and S5c respectively. In blank electrolyte, the charge transfer resistance (R_{ct}) of fresh Mg symmetric cell is as large as 551 kΩ and it even reaches to 1689 kΩ after 50 cycles. In contrast, TPP reduced the R_{ct} of fresh cell to 40 kΩ and that for cycled cell to 152 kΩ. The activation energy of charge transport was calculated

from the fitting parameters of R_{ct} (Tab. S2) by the Arrhenius formula. As shown in Fig. 4c, compared with the high energy barrier (43.6 kJ mol⁻¹) brought by the passivation film in the blank electrolyte, TPP diminishes charge transport activation energy to 16.6 kJ mol⁻¹, indicating that Mg²⁺ have more favorable charge transfer process with the addition of TPP [43]. The better charge transfer kinetics can also be verified by the increase of exchange current density. The Tafel plot of different electrolytes in Fig. 4d reveals a higher exchange current density of the electrolyte with TPP, responding a facilitated Mg²⁺ transport improved by TPP. Based on the electrochemical results above, the introduction of TPP accelerated the charge transfer process and made a significant improvement on anode-electrolyte interphase.

The improvement of the morphology of Mg deposition can also reflect the facilitated Mg²⁺ desolvation process. Fig. 5a-b are the scanning electron microscope (SEM) images of cycled Mg electrodes in different electrolytes. The difference in deposition morphology between the two electrolytes demonstrates the discrepancy in symmetric battery lifespan. In blank electrolyte, the passivation of interphase hampers the deposition of Mg and makes the current unevenly distributed. On this occasion, the plated Mg tends to form spheroidal deposits on the anode and penetrates separators eventually. With the addition of TPP, by contrast, the passivation of anode-electrolyte interphase is alleviated and the current on Mg surface is distributed evenly, smoothing the morphology of Mg deposition and conserves battery life.

To inspect the effect of TPP adsorption on inhibiting side reaction, energy dispersive spectrometer (EDS) analysis of Mg electrode after cycled in different electrolytes are shown in Fig. S6. The Mg electrode cycled in blank electrolyte contains much higher decompose element (C, N, O, F) than the one cycled in TPP-containing electrolyte. The X-ray photoelectron spectroscopy (XPS) was also performed on the cycled Mg

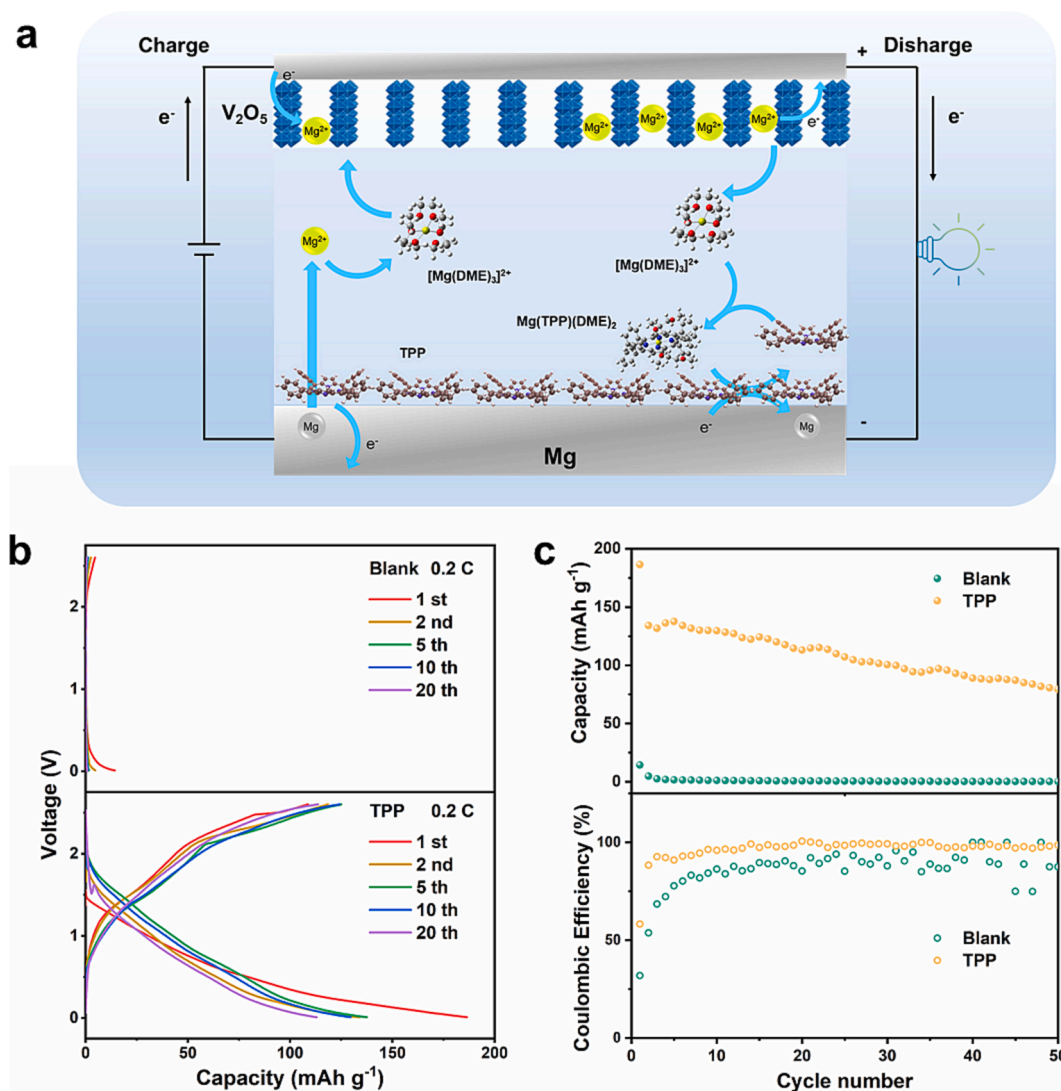


Fig. 6. (a) Schematic illustration of the Mg||V₂O₅ battery charge/discharge process. (b) Charge/discharge profiles and (c) cycling performance of the Mg||V₂O₅ batteries with different electrolytes.

electrodes to investigate the decomposition components, and the results are presented in Fig. 5c-e and Fig. S7. Both decomposition products (MgO, Mg(OH)₂, MgF₂, SO_x and MgS_x) and residual electrolytes can be detected on the surface of cycled Mg. The presence of decomposition products not only implies side reductions on Mg surface, but also causes thicker passivation film to block Mg stripping/plating. In the high-resolution XPS O 1 s spectra in Fig. 5c, the peak at 530.2, 532.0 and 533.0 eV can be assigned to MgO, Mg(OH)₂ and O = S = O, respectively. Among these, O = S = O can be considered as derived from TFSl. The proportion of MgO and Mg(OH)₂ on cycled Mg in the electrolyte with TPP is lower than that for the blank electrolyte, suggesting the alleviation of passivation. Due to oxidation during sample transfer, the reduction in the proportion of MgO and Mg(OH)₂ is not very significant. The peaks at 685.7 and 688.6 eV in Fig. 5d are attributed to MgF₂ in decomposition products and -CF₃ from TFSl, respectively. The proportion of decomposition product MgF₂ is greatly reduced after TPP is added to the electrolyte. Regarding the S 2p spectra (Fig. 5e), in contrast to the blank sample, the peaks of MgS_x (162.2 eV) and SO_x (167.7 eV) exhibit much lower contents in TPP-containing electrolyte. The decrease of decomposition product content on metal surface demonstrates that TPP molecules hinder the decomposition of electrolyte and the formation of passivation film.

The practicability of the TPP additive in Mg metal batteries is

investigated by applying it to a classic Mg||V₂O₅ battery system, as illustrated in Fig. 6a. To facilitate the Mg²⁺ diffusion in V₂O₅, it is a common method to expand the interlayer distance by intercalating other substances [44–46]. The polyaniline (PANI) is chosen to intercalate within V₂O₅ by using a previous reported method [47]. For blank electrolyte, high overpotential of Mg stripping/plating causes the low discharge plateau and high charge plateau of Mg||V₂O₅ batteries (Fig. 6b). In Fig. 6c, with the deterioration of anode/electrolyte interfacial passivation, the specific capacity of Mg||V₂O₅ battery quickly drops to negligible level. In comparison, the addition of TPP renders Mg||V₂O₅ batteries with Mg(TFSl)₂/DME electrolyte cycle smoothly. Mg||V₂O₅ battery shows an initial specific capacity of 186.5 mAh g⁻¹ and remains 79.4 mAh g⁻¹ after 50 cycles, verifying the practicability of the TPP additive in Mg metal batteries. The Mg||V₂O₅ battery in this work is far superior to previously reported Mg metal interfacial optimization based on the Mg(TFSl)₂/DME electrolytes and even competitive with that based on the Mg(TFSl)₂/PC electrolytes (Table S3).

3. Conclusion

In summary, a Cl-free electrolyte additive, TPP, for the Mg(TFSl)₂/DME electrolyte has been developed. With only a small amount of TPP was added to the electrolyte, the polarization voltage of the symmetrical

batteries is reduced to 0.6 V and the lifespan of the symmetrical batteries is extended to more than 500 h. The adsorption of TPP on Mg metal plays a crucial role in diminishing polarization voltage. TPP molecules adsorbed on Mg metal can not only block the direct contact between Mg and passivation-inducing factors, but also create a locally high concentration of TPP. XPS analysis showed that decomposition products on Mg metal were eliminated, verifying the passivation prevention effect of adsorbed TPP molecules and explaining the extremely low stripping overpotential. While the lower plating overpotential is demonstrated by calculating the Gibbs free energy change during desolvation process. It turns out that the $[\text{Mg}(\text{DME})_3]^{2+}$ in blank electrolyte is likely to decompose while $[\text{MgTPP}(\text{DME})_2]$ presenting on the near surface of Mg in TPP-containing electrolyte has higher stability and lower energy barrier during desolvation. $\text{Mg}||\text{V}_2\text{O}_5$ battery with TPP additive exhibits an initial capacity of 186.5 mAh g^{-1} and remains 79.4 mAh g^{-1} after 50 cycles. Our study provides a facile and effective strategy for the application of Cl-free conventional electrolyte in Mg metal batteries and reveals the mechanism of how TPP promotes Mg stripping/plating, which would enlighten the modification of Mg conventional electrolyte in the future.

CRedit authorship contribution statement

Yichao Zhuang: Conceptualization, Data curation, Formal analysis, Methodology, Visualization, Writing – original draft. **Jiayue Wu:** Data curation, Resources, Validation, Writing – review & editing. **Haiming Hua:** Resources, Validation, Writing – review & editing. **Fei Wang:** Validation, Writing – review & editing. **Dongzheng Wu:** Validation, Writing – review & editing. **Yaoqi Xu:** Validation. **Jing Zeng:** Funding acquisition, Project administration, Writing – review & editing. **Jinbao Zhao:** Funding acquisition, Supervision, Writing – review & editing.

Declaration of competing interest

The authors declare that they have no known competing financial interests or personal relationships that could have appeared to influence the work reported in this paper.

Data availability

No data was used for the research described in the article.

Acknowledgments

The authors gratefully acknowledge the National Natural Science Foundation of China (Nos. 21875198, 22005257, and 22021001), the Natural Science Foundation of Fujian Province of China (No. 2020J05009) for financial support. We are grateful to Dr. Gaowa Liu at Tan Kah Kee Innovation Laboratory (IKKEM), Center for Micronano Fabrication and Advanced Characterization, Xiamen University, for help with the XPS measurement. Numerical computations were performed on Hefei advanced computing center.

Appendix A. Supplementary data

Supplementary data to this article can be found online at <https://doi.org/10.1016/j.cej.2023.148170>.

References

- [1] R.C. Massé, E. Uchaker, G. Cao, Beyond Li-ion: electrode materials for sodium- and magnesium-ion batteries, *Sci. China Mater.* 58 (9) (2015) 715–766, <https://doi.org/10.1007/s40843-015-0084-8>.
- [2] J.W. Choi, D. Aurbach, Promise and reality of post-lithium-ion batteries with high energy densities, *Nat. Rev. Mater.* 1 (4) (2016) 16013, <https://doi.org/10.1038/natrevmats.2016.13>.
- [3] F. Ming, H. Liang, G. Huang, Z. Bayhan, H.N. Alshareef, MXenes for Rechargeable Batteries Beyond the Lithium-Ion, *Adv. Mater.* 33 (1) (2020) 2004039, <https://doi.org/10.1002/adma.202004039>.
- [4] D. Li, Y. Yuan, J. Liu, M. Fichtner, F. Pan, A review on current anode materials for rechargeable Mg batteries, *J. Magnes. Alloy.* 8 (4) (2020) 963–979, <https://doi.org/10.1016/j.jma.2020.09.017>.
- [5] H.D. Yoo, I. Shterenberg, Y. Gofer, G. Gershtinsky, N. Pour, D. Aurbach, Mg rechargeable batteries: an on-going challenge, *Energy Environ. Sci.* 6 (8) (2013) 2265–2279, <https://doi.org/10.1039/c3ee40871j>.
- [6] C.B. Bucur, T. Gregory, A.G. Oliver, J. Muldoon, Confession of a Magnesium Battery, *J. Phys. Chem. Lett.* 6 (18) (2015) 3578–3591, <https://doi.org/10.1021/acs.jpclett.5b01219>.
- [7] F. Liu, T. Wang, X. Liu, L.Z. Fan, Challenges and Recent Progress on Key Materials for Rechargeable Magnesium Batteries, *Adv. Energy Mater.* 11 (2) (2020) 2000787, <https://doi.org/10.1002/aenm.202000787>.
- [8] C. You, X. Wu, X. Yuan, Y. Chen, L. Liu, Y. Zhu, L. Fu, Y. Wu, Y.-G. Guo, T. van Ree, Advances in rechargeable Mg batteries, *J. Mater. Chem. A* 8 (48) (2020) 25601–25625, <https://doi.org/10.1039/d0ta09330k>.
- [9] R. Mohtadi, O. Tutusaus, T.S. Arthur, Z. Zhao-Karger, M. Fichtner, The metamorphosis of rechargeable magnesium batteries, *Joule* 5 (3) (2021) 581–617, <https://doi.org/10.1016/j.joule.2020.12.021>.
- [10] C. Song, F. Shuang, L. Henan, S. Yumeng, Y. Hui Ying, Recent advances in kinetic optimizations of cathode materials for rechargeable magnesium batteries, *Coord. Chem. Rev.* 466 (2022), 214597, <https://doi.org/10.1016/j.ccr.2022.214597>.
- [11] Y. Li, Y. Zheng, K. Guo, J. Zhao, C. Li, Mg-Li Hybrid Batteries: The Combination of Fast Kinetics and Reduced Overpotential, *Energy Mater. Adv.* (2022), <https://doi.org/10.34133/2022/9840837>.
- [12] Z. Jinlei, L. Jing, W. Min, Z. Zhonghua, Z. Zhenfang, C. Xi, D. Aobing, D. Shanmu, L. Zhenjiang, L. Guicun, C. Guanglei, The origin of anode-electrolyte interfacial passivation in rechargeable Mg-metal batteries, *Energy Environ. Sci.* 16 (3) (2023) 1111–1124, <https://doi.org/10.1039/d2ee03270h>.
- [13] N.N. Rajput, X. Qu, N. Sa, A.K. Burrell, K.A. Persson, The Coupling between Stability and Ion Pair Formation in Magnesium Electrolytes from First-Principles Quantum Mechanics and Classical Molecular Dynamics, *J. Am. Chem. Soc.* 137 (9) (2015) 3411–3420, <https://doi.org/10.1021/jacs.5b01004>.
- [14] T.J. Seguin, N.T. Hahn, K.R. Zavadil, K.A. Persson, Elucidating Non-aqueous Solvent Stability and Associated Decomposition Mechanisms for Mg Energy Storage Applications From First-Principles, *Front. Chem.* 7 (2019) 175, <https://doi.org/10.3389/fchem.2019.00175>.
- [15] W. Fei, H. Haiming, W. Dongzheng, L. Jialin, X. Yaoqi, N. Xianzhen, Z. Yichao, Z. Jing, Z. Jinbao, Solvent Molecule Design Enables Excellent Charge Transfer Kinetics for a Magnesium Metal Anode, *ACS Energy Lett.* 8 (1) (2022) 780–789, <https://doi.org/10.1021/acseenergylett.2c02525>.
- [16] Y. Yu, A. Baskin, C. Valero-Vidal, N.T. Hahn, Q. Liu, K.R. Zavadil, B.W. Eichhorn, D. Prendergast, E.J. Crumlin, Instability at the Electrode/Electrolyte Interface Induced by Hard Cation Chelation and Nucleophilic Attack, *Chem. Mater.* 29 (19) (2017) 8504–8512, <https://doi.org/10.1021/acs.chemmater.7b03404>.
- [17] L. Zhiming, B. Chunmei, Strategies to Enable Reversible Magnesium Electrochemistry: From Electrolytes to Artificial Solid-Electrolyte Interphases, *Angew. Chem. Int. Ed.* 60 (20) (2020) 11036–11047, <https://doi.org/10.1002/anie.202006472>.
- [18] S. Yue, A. Fei, L. Yi-Chun, Electrolyte and Interphase Design for Magnesium Anode: Major Challenges and Perspectives, *Small* 18 (43) (2022) 2200009, <https://doi.org/10.1002/sml.202200009>.
- [19] M. Toshihiko, W. Mariko, Oxygen – A Fatal Impurity for Reversible Magnesium Deposition/Dissolution, *J. Mater. Chem. A* 11 (18) (2023) 9755–9761, <https://doi.org/10.1039/d3ta01286g>.
- [20] D. Aurbach, Z. Lu, A. Schechter, Y. Gofer, H. Gizbar, R. Turgeman, Y. Cohen, M. Moshkovich, E. Levi, Prototype systems for rechargeable magnesium batteries, *Nature* 407 (6805) (2000) 724–727, <https://doi.org/10.1038/35037553>.
- [21] J.G. Connell, B. Genorio, P.P. Lopes, D. Strmcnik, V.R. Stamenkovic, N. M. Markovic, Tuning the Reversibility of Mg Anodes via Controlled Surface Passivation by $\text{H}_2\text{O}/\text{Cl}^-$ in Organic Electrolytes, *Chem. Mater.* 28 (22) (2016) 8268–8277, <https://doi.org/10.1021/acs.chemmater.6b03227>.
- [22] A. Doron, G. Haim, S. Alex, C. Orit, E.G. Hugo, G. Yossi, G. Israel, Electrolyte Solutions for Rechargeable Magnesium Batteries Based on Organomagnesium Chloroaluminate Complexes, *J. Electrochem. Soc.* 149 (2) (2019) A115–A121, <https://doi.org/10.1149/1.1429925>.
- [23] S. Yagi, A. Tanaka, Y. Ichikawa, T. Ichitsubo, E. Matsubara, Electrochemical Stability of Magnesium Battery Current Collectors in a Grignard Reagent-Based Electrolyte, *J. Electrochem. Soc.* 160 (3) (2013) C83–C88, <https://doi.org/10.1149/2.033303jes>.
- [24] S. Chakrabarty, J.A. Blázquez, T. Sharabani, A. Maddegalla, O. Leonet, I. Urdampilleta, D. Sharon, M. Noked, A. Mukherjee, Stability of Current Collectors Against Corrosion in APC Electrolyte for Rechargeable Mg Battery, *J. Electrochem. Soc.* 16 (8) (2021), 080526, <https://doi.org/10.1149/1945-7111/ac1cc8>.
- [25] L.F. Wan, B.R. Perdue, C.A. Appleby, D. Prendergast, Mg Desolvation and Intercalation Mechanism at the Mo6S8 Chevrel Phase Surface, *Chem. Mater.* 27 (17) (2015) 5932–5940, <https://doi.org/10.1021/acs.chemmater.5b01907>.
- [26] S. Seoung-Bum, G. Tao, P.H. Steve, K.X. Steirer, S. Adam, N. Andrew, W. Chunsheng, C. Arthur, X. Kang, B. Chunmei, An artificial interphase enables reversible magnesium chemistry in carbonate electrolytes, *Nat. Chem.* 10 (5) (2018) 532–539, <https://doi.org/10.1038/s41557-018-0019-6>.
- [27] Z. Yijie, L. Jiang, Z. Wanyu, D. Huanglin, Z. Xiaoli, L. Yuan, Z. Bowen, Y. Xiaowei, Defect-Free Metal-Organic Framework Membrane for Precise Ion/Solvent

- Separation toward Highly Stable Magnesium Metal Anode, *Adv. Mater.* 34 (6) (2021) 2108114, <https://doi.org/10.1002/adma.202108114>.
- [28] P. Clément, H. Arthur, L. Jean-Bernard, F. Dominique, A. Joachim, C. Jean-Noel, L. Olivera, B. Jan, D. Robert, D. Rémi, F. Jean-Sebastien, S. Lorenzo, B. Romain, Alloying electrode coatings towards better magnesium batteries, *J. Mater. Chem. A* 10 (22) (2022) 12104–12113, <https://doi.org/10.1039/d2ta02083a>.
- [29] P. Clément, L. Jean-Bernard, A. Joachim, D. Rémi, S. Lorenzo, B. Romain, Surface Amalgam on Magnesium Electrode: Protective Coating or Not? *Energy Technol.* 11 (1) (2022) 2201098, <https://doi.org/10.1002/ente.202201098>.
- [30] H. Ye Yeong, L. Nam Kyeong, P. Sol Hui, S. Jisu, L. Yun Jung, TFSI Anion Grafted Polymer as an Ion-Conducting Protective Layer on Magnesium Metal for Rechargeable Magnesium Batteries, *Energy Storage Mater.* 51 (2022) 108–121, <https://doi.org/10.1016/j.ensm.2022.06.014>.
- [31] Y. Li, X. Zhou, J. Hu, Y. Zheng, M. Huang, K. Guo, C. Li, Reversible Mg metal anode in conventional electrolyte enabled by durable heterogeneous SEI with low surface diffusion barrier, *Energy Storage Mater.* 46 (2021) 1–9, <https://doi.org/10.1016/j.ensm.2021.12.023>.
- [32] Y. Zhuang, D. Wu, F. Wang, Y. Xu, J. Zeng, J. Zhao, Tailoring a Hybrid Functional Layer for Mg Metal Anodes in Conventional Electrolytes with a Low Overpotential, *ACS Appl. Mater. Interfaces* 14 (42) (2022) 47605–47615, <https://doi.org/10.1021/acsmi.2c11911>.
- [33] Y. Sun, Q. Zou, W. Wang, Y.-C. Lu, Non-passivating Anion Adsorption Enables Reversible Magnesium Redox in Simple Non-nucleophilic Electrolytes, *ACS Energy Lett.* 6 (10) (2021) 3607–3613, <https://doi.org/10.1021/acscenergylett.1c01780>.
- [34] W. Jiahe, Z. Wanyu, D. Huanglin, W. Bingxin, Z. Yijie, L. Wanfei, Z. Xiaoli, Y. Xiaowei, Electrostatic Shielding Guides Lateral Deposition for Stable Interphase toward Reversible Magnesium Metal Anodes, *ACS Appl. Mater. Interfaces* 12 (17) (2020) 19601–19606, <https://doi.org/10.1021/acsmi.0c03603>.
- [35] L. Yuan, Z. Wanyu, P. Zhenghui, F. Zhengqing, Z. Meng, Z. Xiaoli, C. Jianping, Y. Xiaowei, Interfacial Engineering of Magnesiophilic Coordination Layer Stabilizes Mg Metal Anode, *Angew. Chem. Int. Ed.* 62 (25) (2023) e202302617.
- [36] H. Singyuk, J. Xiao, G. Karen, W. Peng-fei, W. Luning, X. Jijian, S. Ruimin, B. Oleg, W. Chunsheng, Solvation sheath reorganization enables divalent metal batteries with fast interfacial charge transfer kinetics, *Science* 374 (6564) (2021) 172–178, <https://doi.org/10.1126/science.abg3954>.
- [37] Z. Wanyu, P. Zhenghui, Z. Yijie, L. Yuan, D. Huanglin, S. Yayun, Z. Zhijun, Z. Bowen, C. Jianping, Z. Xiaoli, Y. Xiaowei, Tailoring Coordination in Conventional Ether-based Electrolytes for Reversible Magnesium Metal Anodes, *Angew. Chem. Int. Ed.* 61 (30) (2022) e202205187.
- [38] M. Polakovic, T. Gorner, F. Villieras, P. de Donato, J.L. Bersillon, Kinetics of salicylic acid adsorption on activated carbon, *Langmuir* 21 (7) (2005) 2988–2996, <https://doi.org/10.1021/la047143+>.
- [39] J. Zhang, J. Bai, M. Duan, J. Yang, L. Bian, Derivation of adsorption capacity and adsorption isotherm by a single adsorbate concentration in liquid–solid system, *Chem. Pap.* 75 (6) (2021) 2459–2476, <https://doi.org/10.1007/s11696-020-01476-9>.
- [40] P. Hyeokjun, L. Hyung-Kyu, O. Si Hyoung, P. Jooha, L. Hee-Dae, K. Kisuk, Tailoring Ion-Conducting Interphases on Magnesium Metals for High-Efficiency Rechargeable Magnesium Metal Batteries, *ACS Energy Lett.* 5 (12) (2020) 3733–3740, <https://doi.org/10.1021/acscenergylett.0c02102>.
- [41] H. Dai, J. Dong, M. Wu, Q. Hu, D. Wang, L. Zuin, N. Chen, C. Lai, G. Zhang, S. Sun, Cobalt-Phthalocyanine-Derived Molecular Isolation Layer for Highly Stable Lithium Anode, *Angew. Chem. Int. Ed.* 60 (36) (2021) 19852–19859, <https://doi.org/10.1002/anie.202106027>.
- [42] V. Lockett, R. Sedev, J. Ralston, M. Horne, T. Rodopoulos, Differential Capacitance of the Electrical Double Layer in Imidazolium-Based Ionic Liquids: Influence of Potential, Cation Size, and Temperature, *J. Phys. Chem. C* 112 (19) (2008) 7486–7495, <https://doi.org/10.1021/jp7100732>.
- [43] Z. Rupeng, C. Can, L. Ruinan, L. Yaqi, D. Chunyu, G. Yunzhi, H. Hua, M. Yulin, Z. Pengjian, Y. Geping, An Artificial Interphase Enables the Use of Mg(TFSI)₂-Based Electrolytes in Magnesium Metal Batteries, *Chem. Eng. J.* 426 (2021), 130751, <https://doi.org/10.1016/j.cej.2021.130751>.
- [44] D. Wu, J. Zeng, H. Hua, J. Wu, Y. Yang, J. Zhao, NaV6O15: A promising cathode material for insertion/extraction of Mg²⁺ with excellent cycling performance, *Nano Research* 13 (2) (2020) 335–343, <https://doi.org/10.1007/s12274-019-2602-6>.
- [45] J. Tian, X. Zhou, Q. Wu, C. Li, Li-salt mediated Mg-rhodizonate batteries based on ultra-large cathode grains enabled by K-ion pillaring, *Energy Storage Mater.* 22 (2019) 218–227, <https://doi.org/10.1016/j.ensm.2019.01.019>.
- [46] Z. Yao, Y. Yu, Q. Wu, M. Cui, X. Zhou, J. Liu, C. Li, Maximizing Magnesium Capacity of Nanowire Cluster Oxides by Conductive Macromolecule Pillaring and Multication Intercalation, *Small* 17 (30) (2021) 2102168, <https://doi.org/10.1002/sml.202102168>.
- [47] S. Liu, H. Zhu, B. Zhang, G. Li, H. Zhu, Y. Ren, H. Geng, Y. Yang, Q. Liu, C.C. Li, Tuning the Kinetics of Zinc-Ion Insertion/Extraction in V₂O₅ by In Situ Polyaniline Intercalation Enables Improved Aqueous Zinc-Ion Storage Performance, *Adv. Mater.* 32 (26) (2020) 2001113, <https://doi.org/10.1002/adma.202001113>.